6.7

LIFECYCLE ANALYSIS OF CUMULUS CLOUDS USING A 3D VIRTUAL REALITY ENVIRONMENT

Thijs Heus,* Harm J.J. Jonker,
Mult-Scale Physics, Delft University of Technology, The Netherlands
Eric J. Griffith and Frits H. Post,
Data Visualization Group, Faculty of Electrical Engineering, Mathematics and Computer Science,
Delft University of Technology, The Netherlands

1. INTRODUCTION

The aim of this study is to study shallow cumulus clouds evolving through their entire life cycle using Large Eddy Simulations. Although LES is an enriching tool to study the physics of the cloudy boundary layer, its completeness also poses a problem; high-resolution, three-dimensional time-dependent datasets are often too large for even state-of-the-art equipment to explore. This proves especially to be a problem when one wants to explore the variation of the data in time, e.g. the evolution of a cloud from birth to a (apparent) steady-state mature phase and onwards until the decay of the cloud, since the entire 4D dataset has to be evaluated at once. Furthermore, in contrast with time independent evaluation of cloud fields, the definition of a single cloud moving in time turns out to be much harder since the distinction between a collision of two separate clouds and a single cloud that loses or acquires a few chunks is hard to capture in absolute rules, which especially poses a problem in the onset or decay of a cloud, where a cloud often consists of several small pieces. However, it turns out that the human perception is well suited to discern those different situations, which suggests a carefull selection of clouds by visual inspection as performed by (Zhao and Austin, 2005). Close inspection of this interesting paper suggested that their method was not perfect yet; selection of appropriate clouds turned out to be difficult, which resulted in the selection of 6 clouds. Keeping in mind that three of those six clouds were small and three were large, it becomes clear that judgment on a statistical basis needed improvement.

In this paper we attempt to enhance this selection method by involving a Virtual Reality Environment (VE) to visualize the system in three dimensions, thus showing the cloud field in a more realistic way as well as taking advantage of the fact that our vision is very much used to 3D, time-evolving images. After extracting a sizeable number of clouds from the simulations, clouds can be examined on an individual basis while resulting hypotheses can be tested on other species and serve as a basis to make some general conclusions on the properties of clouds in their respective life stages - which could be compared with the experiences of trained observationalists who can easily distinguish a cloud in its infancy from a fading one.

Corresponding author address: Thijs Heus, Dept. of Multi-Scale Physics, Delft University of Technology, Lorentzweg 1, 2628CJ Delft, The Netherlands, e-mail: t.heus@tudelft.nl

2. EXPERIMENTAL SETUP

Using a parallelized version of the LES described by (Cuijpers and Duynkerke, 1993) 7 runs of 7 hours each (with different initial perturbations) are performed based on the BOMEX case (see (Siebesma et al., 2003)). Simulations were done on a $6.4 \times 6.4 \times 3.2 km$ domain with a resolution of $\Delta x = \Delta y = 1.25\Delta z = 25m$. From the seven hours of simulation the first 3 are discarded as spin up and neglected. Every 6 seconds the complete u, v, w, θ_l, q_t and q_l fields are written to disk so that clouds with a (typical) life span of $1800s$ will be captured with 300 points in time.

The used VE is described in detail by (Griffith et al., 2005). To visualize the clouds, all gridpoints that are neighbors (taking the horizontal periodic boundary conditions into account) in space-time are considered to be of the same cloud system and labeled that way. Since this process requires browsing through the entire $40GB$ sized datafield, this cannot be done during visualization but needs to be done in preprocessing. In the VE clouds are visualized by depicting the $q_l = 0$ isosurface, while a 2D graph shows the evolution of the mass of the selected cloud. Cloud systems that already exist at $t = 3h$ or are still active at $t = 7h$ can be disregarded. In figure 1, a simulation of the VE setup is shown.
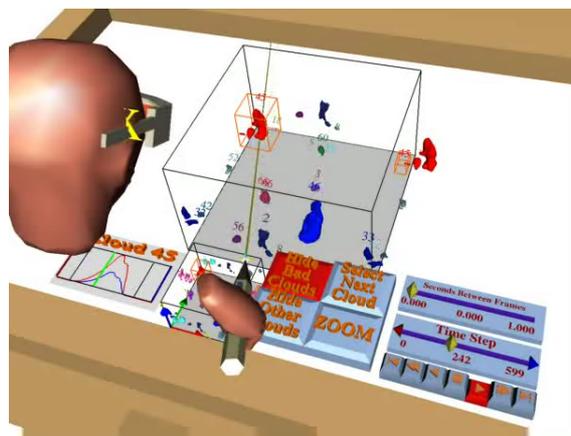

FIG. 1: Overview of the Virtual Environment. The cloudfield can be rotated, zoomed in upon and browsed through in time. By selecting individual clouds, more information becomes available (e.g. the volume as a function of time)

3. CLOUD SELECTION

Using the VE to browse through the data, active cumulus clouds are selected that during the bulk of their lifetime consist of a clear main body with possibly a few chunks broken off. This criterion works rather well during the inspection; the identification by the observer of several seemingly independent clouds which are nevertheless labeled as the same system turned out to be an efficient criterion to dismiss a system. Although the focus lies on clouds with reasonable life spans, it was attempted not to make selections on other criteria (e.g. size or height). Using this method for all five datasets, 40 clouds were selected, yielding sufficient chance for reliable statistics.
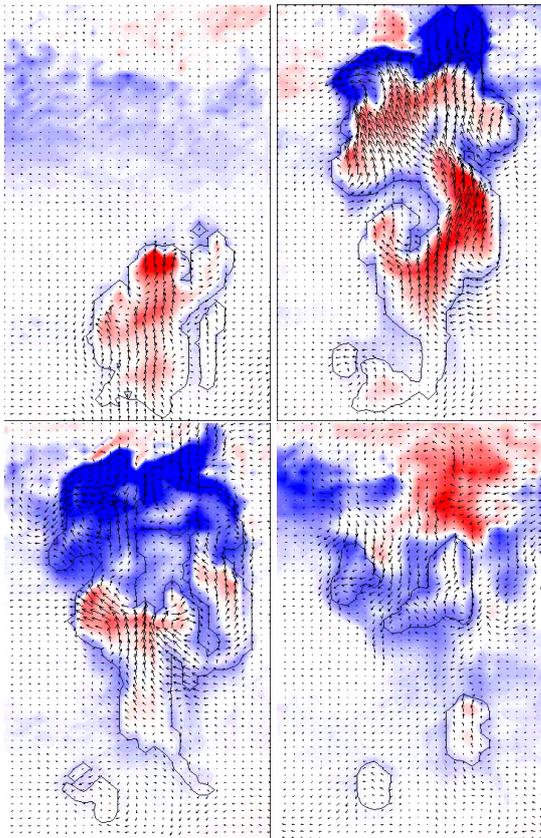
4. RESULTS

FIG. 2: Cross section through the center of mass of a cloud as a function of time. The cloud edge is represented by the solid line, the vector field depicts the in-plane velocity and the color denotes the buoyancy excess. From top to bottom, left to right: Initial growth at $t = 648s$, a mature cloud at $t = 948s$, the detachment of cloudbase at $t = 1074s$ and the dissipating passive remnants at $t = 1236s$

In figure 2, a cross section through the center of mass of one of the selected clouds is shown at several points in time, with the colorscale denoting the buoyancy excess. In view of this study, a few things can be noticed immediately: during the growth phase for instance, slightly below the top of the cloud an area of high buoyancy can be seen seemingly pushing the cloud-top interface upwards and sucking along the air beneath. Furthermore, at $t = 948s$ recirculation patterns as observed for instance by (Blyth, 1993) are clearly visable re-entering the cloud just below the buoyancy front. At the end of the final pulse, the cloud leaves its base level and breaks up in several pieces that finally dissolve.

In figure 3 the amount of q_l, θ_l and w integrated over an $x - y$ plane of the cloud are shown as a function of height and time. In all plots, the way the cloud grows is immediately striking. Even after the cloud reaches the inversion height, this process repeats itself several times, displaying the pulsating growth also found by (Zhao and Austin, 2005). The increased liquid water content inside such a bubble would also result in less transparent and sharper cloud edges; this lack of 'silver lining' is usually a key for observationalists to distinguish an active from a decaying cloud.

From the integrated vertical velocity diagram it is clear that the front of a pulse is advancing the fastest; below the top, velocities are much lower and even negative, indicating air detaching from the bubble, which can hamper the advance of the following thermal as can be seen for instance around $t = 1620$. This is also particularly visible in the decay phase; while the final thermal is rising and the cloud detaches from cloudbase, the strongest negative velocities are located at the bottom of the cloud; apparently, this is the place where the cloud mixes with the environment and dissipates.

The overshoot at inversion height is reflected by the sharp gradient at cloud-top. Zooming in at cloudbase, in figure 4 the lateral integrated total water content q_t at cloudbase is depicted. Here the fingerprint of the pulses is visible as well, but, rather interestingly, the peak in q_t seems to be at the start of the pulse. This behavior is confirmed for another cloud in figure 5. One could understand this by supposing that some kind of threshold total water content is needed to trigger a thermal to shoot upwards through the cloud, hence allowing entrainment to dry out the cloudbase, which eventually shuts down the pulse as well as the lateral entrainment. From here, the lack of activity allows the subcloud thermal to refill the moist buffer.

5. OUTLOOK

Up to now, a phenomenological approach was used to study the individual clouds. The future aim of this study is to capture these phenomena in a statistical way, using the database of 40 clouds to gain reliable statistics. To do this, more understanding of the timescale on which the pulsating growth operate is needed.
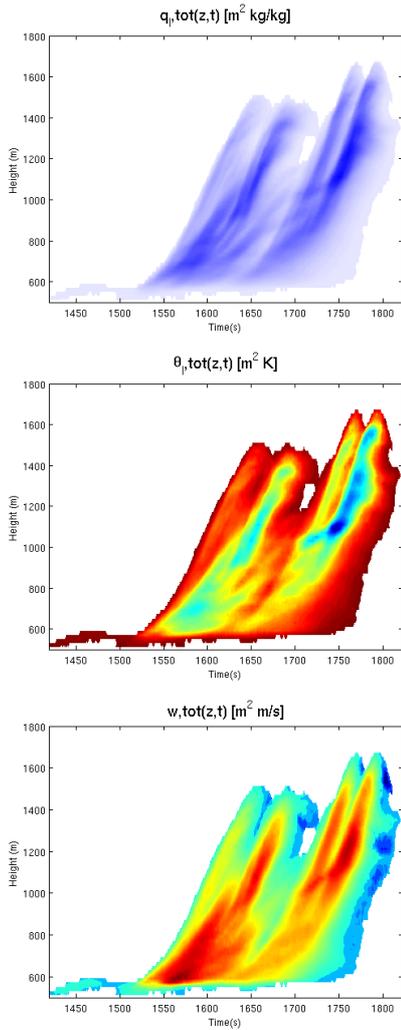
6. ACKNOWLEDGMENTS

FIG. 3: The lateral integrated amounts ($\int \int \varphi dx dy$) of $\varphi = q_l, \theta_l, w$ (from top to bottom) as a function of height and time.
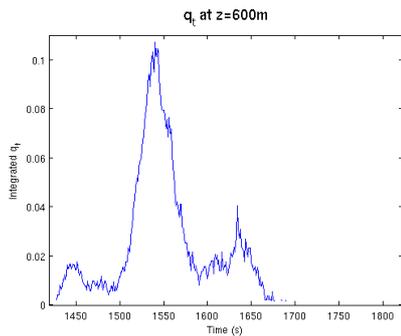

FIG. 4: $q_t(z = 600m, t)$. In comparison with figure 3 one clearly sees a peak in q_t at the onset of a pulse.
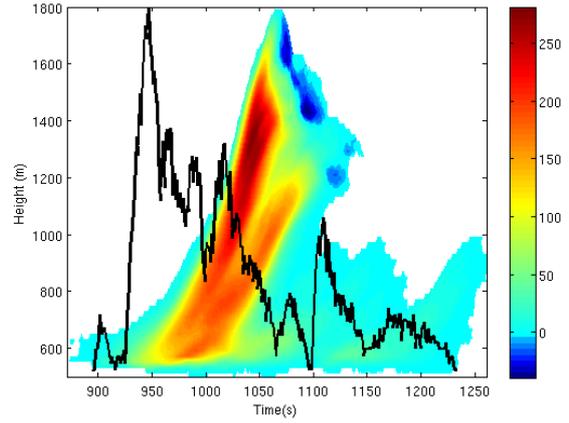

FIG. 5: For a different cloud $w(z, t)$ and $q_t(cloudbase, t)$ diagrams, again showing the build up of moist before the start of a pulse.

REFERENCES

Blyth, A. M., 1993: Entrainment in cumulus clouds. *Journal of Applied Meteorology*, **32**, 626–641.

Cuijpers, J. and P. Duynkerke, 1993: Large-eddy simulation of trade wind cumulus clouds. *Journal of the Atmospheric Sciences*, **50**, 3894–3908.

Griffith, E. J., F. H. Post, M. Koutek, T. Heus, and H. J. J. Jonker, 2005: Feature tracking in VR for cumulus cloud life-cycle studies. In *Virtual Environments 2005*, Kjems, E. and Blach, R., editors, 121–128.

Siebesma, A. P., C. S. Bretherton, A. Brown, A. Chlond, J. Cuxart, P. G. Duynkerke, H. L. Jiang, M. Khairoutdinov, D. Lewellen, C. H. Moeng, E. Sanchez, B. Stevens, and D. E. Stevens, 2003: A large eddy simulation intercomparison study of shallow cumulus convection. *Journal of the Atmospheric Sciences*, **60**(10), 1201–1219.

Zhao, M. and P. Austin, 2005: Life cycle of numerically simulated shallow cumulus clouds. part I: Transport. *Journal of the Atmospheric Sciences*, **62**, 1269–1290.